

Formation and hydrogenation of $p(2 \times 2)$ -N on Pt(111)

Eldad Herceg, James Jones, Kumudu Mudiyansele, Michael Trenary*

Department of Chemistry, University of Illinois at Chicago, 845 West Taylor Street, Chicago, IL 60607-7061, United States

Received 14 March 2006; accepted for publication 14 July 2006

Available online 8 August 2006

Abstract

The formation of a well-ordered $p(2 \times 2)$ overlayer of atomic nitrogen on the Pt(111) surface and its reaction with hydrogen were characterized with reflection absorption infrared spectroscopy (RAIRS), temperature programmed desorption (TPD), low energy electron diffraction (LEED), Auger electron spectroscopy (AES), and X-ray photoelectron spectroscopy (XPS). The $p(2 \times 2)$ -N overlayer is formed by exposure of ammonia to a surface at 85 K that is covered with 0.44 monolayer (ML) of molecular oxygen and then heating to 400 K. The reaction between ammonia and oxygen produces water, which desorbs below 400 K. The only desorption product observed above 400 K is molecular nitrogen, which has a peak desorption temperature of 453 K. The absence of oxygen after the 400 K anneal is confirmed with AES. Although atomic nitrogen can also be produced on the surface through the reaction of ammonia with an atomic, rather than molecular, oxygen overlayer at a saturation coverage of 0.25 ML, the yield of surface nitrogen is significantly less, as indicated by the N_2 TPD peak area. Atomic nitrogen readily reacts with hydrogen to produce the NH species, which is characterized with RAIRS by an intense and narrow (FWHM $\sim 4 \text{ cm}^{-1}$) peak at 3322 cm^{-1} . The areas of the H_2 TPD peak associated with NH dissociation and the XPS N 1s peak associated with the NH species indicate that not all of the surface N atoms can be converted to NH by the methods used here.

© 2006 Elsevier B.V. All rights reserved.

Keywords: Ammonia; Oxygen; Nitrogen; Hydrogen; Platinum; Infrared absorption spectroscopy; Low energy electron diffraction; Thermal desorption spectroscopy

1. Introduction

The properties of atomic nitrogen on platinum surfaces are relevant to several important catalytic processes. These include the reduction of NO_x by automotive catalytic converters and the industrial synthesis of nitric oxide through the catalytic oxidation of ammonia [1]. While the formation of molecular nitrogen through oxydehydrogenation of ammonia is an unwanted reaction in nitric acid synthesis, it is the desired product in the catalytic reduction of nitrogen oxides. Two primary objectives motivated the study reported here. First, we wished to establish a simple procedure to produce a clean, well-ordered overlayer of atomic nitrogen on Pt(111). Such a procedure provides a

first step for subsequent studies aimed at establishing the surface chemical properties of this important species, such as its hydrogenation activity. Second, the work also provides new insights into the important ammonia oxydehydrogenation reaction on platinum surfaces.

The reaction between oxygen and ammonia has been investigated on many metallic surfaces including ruthenium [2,3], rhodium [4,5], iridium [6–8], nickel [9,10], copper [11–13], and other metals [5,14–16]. Platinum surfaces have been also widely explored and studies have been carried out on supported Pt [17–19], polycrystalline Pt [5,20–26], and single-crystal Pt [21,27–35]. In the mid-1960s, Fogel et al. [36] proposed a reaction scheme in which N_2 is formed in a bimolecular surface reaction between NO and NH_3 , whereas NO is formed by a one-step mechanism from the $NH_3 + O_2$ and/or $NH_3 + O$ reactions. Although an imide radical mechanism was inferred, Fogel et al. failed to detect any intermediates using secondary ion mass

* Corresponding author. Tel.: +1 312 996 0777; fax: +1 312 996 0431.
E-mail address: mtrenary@uic.edu (M. Trenary).

spectrometry. Kinetic studies [5,22] over the pressure range 0.1–1.0 Torr showed that the reaction rates observed can be described by several Langmuir–Hinshelwood rate expressions based on the chemical reactions given above. This was further supported by studies performed by Nutt and Kapur [20]. The models explaining the overall reaction mechanism [5,20,27,28] have combined the findings by Fogel et al. with steps involving the competition for active sites between NH_3 , O_2 , and the NO intermediate. However, these models do not provide any details of the elementary reaction steps.

Ultra high vacuum (UHV) steady-state reaction studies by Gland and Korchak [27] on stepped Pt(S)-12(111) × (111) have shown that the product content is strongly influenced by substrate temperature and reactant composition. Excess O_2 and temperatures above ~ 650 K favor production of NO, while excess NH_3 and temperatures between 400 and 650 K result in N_2 production [27]. It was concluded that step edges are the most active catalytic sites, which was further confirmed by comparison of results obtained on Pt(111) [28]. Interestingly, they used AES to show that below ~ 650 K a nitrogenic surface species is the only adsorbate, although this species was not identified. This supports the idea of formation of N_2 without invoking NO as an intermediate, which contradicts the models referred to above. The insignificance of the $\text{NH}_3 + \text{NO}$ reaction in NH_3 oxidation can also be seen from the absence of any reaction between these two species coadsorbed on Pt(111) under UHV [37,38]. To account for the production of NH and OH radicals over polycrystalline Pt as detected by laser induced fluorescence, Selwyn and Lin [23] proposed that atomic and radical species should be considered. Recent work on Pt(111) [29,32] also has led to consideration of different mechanisms of NO formation, such as $\text{N} + \text{O} \rightarrow \text{NO}$ recombination and $\text{NH} + \text{O} \rightarrow \text{NO} + \text{H}$ exchange. In these schemes, molecular nitrogen is formed via recombination of N atoms. Mierher and Ho identified NH, NH_2 , and OH as intermediate species on Pt(111) using electron energy loss spectroscopy (EELS) [32]. They concluded that NH_3 is activated through the stripping of one or several H atoms by O or OH followed by the $\text{N} + \text{O}$ reaction to form NO and the $\text{N} + \text{N}$ reaction to form N_2 . This reaction picture was further supported by theoretical calculations [39].

The work presented here offers new information on the oxydehydrogenation of NH_3 under UHV conditions. We confirm many of the previous findings from Ref. [32] and find that N_2 is definitely formed from the combination of surface N atoms. In addition, we present spectroscopic evidence for the reaction of NH_3 with adsorbed molecular O_2 at 85 K. The reaction with molecular oxygen provides a simple route to the preparation of a well-ordered $\text{p}(2 \times 2)$ -N layer that is free of oxygen. We find that this atomic nitrogen layer readily reacts with hydrogen to form the NH species, although it appears that only a fraction of the N layer can be converted to NH. Formation of a $\text{p}(2 \times 2)$ -N structure on Pt(111) has been reported previ-

ously [31,32], but not its reactivity towards hydrogen. However, our study differs from this earlier study in several ways as described below. The effect of different ammonia exposures on the overall surface chemistry for Pt(111) surfaces saturated with molecular O_2 and atomic O has also been explored. In addition, we find that higher coverages of both N and NH can be formed through the ammonia oxydehydrogenation reactions described here than can be formed through a method we recently described [40] involving electron-induced NH_3 dissociation on Pt(111).

2. Experimental

The results were obtained in two separate UHV chambers using two different Pt(111) crystals. The X-ray photoelectron spectroscopy (XPS) results were obtained in a chamber (chamber 1) with a base pressure of $\sim 2 \times 10^{-10}$ Torr. The system has been described in detail elsewhere [41]. In brief, the UHV chamber is equipped with low energy electron diffraction (LEED), an XPS system, a quadrupole mass spectrometer (QMS) for TPD, and with a Fourier transform infrared (FTIR) spectrometer for reflection absorption infrared spectroscopy (RAIRS) studies. The XPS system consists of a VG CLAM2 hemispherical analyzer and dual anode X-ray source. Mg $\text{K}\alpha$ radiation was used for the XPS study and the spectrometer was calibrated with the $\text{Pt}4f_{7/2}$ peak at a binding energy of 71.2 eV. All TPD, RAIRS, and AES experiments were performed in a second chamber (chamber 2) with a base pressure of $\sim 1 \times 10^{-10}$ Torr. A detailed description of this system can be found elsewhere [42]. In brief, it consists of a stainless steel UHV chamber equipped for AES, LEED, and TPD experiments with a QMS. The chamber is coupled to a commercial Fourier transform infrared (FTIR) spectrometer, a Bruker IFS 66 v/S. The IR beam enters and exits the UHV chamber through differentially pumped O-ring sealed KBr windows and passes through a polarizer before reaching the infrared detector. To achieve maximum sensitivity, an InSb detector was used with a tungsten source for the spectral region above 2500 cm^{-1} , while an MCT (HgCdTe) detector was used with a SiC source for the lower wavenumber region. In cases where the sample was annealed to a temperature above 85 K, the sample was then cooled back to 85 K before the spectrum was acquired. The background reference spectrum was also taken at 85 K. A resolution of 2 cm^{-1} was used for the spectra above 2500 cm^{-1} and 4 cm^{-1} was used for the lower wavenumber region. For the TPD results, signal from the QMS was recorded for each mass at a temperature interval of approximately every 2 K. The data was smoothed using the Savitzky–Golay method with 1.5% of the data points used near each point. The smoothed TPD peak positions can be determined with a precision of ± 1 K, which is also the accuracy of the temperature measurement. The Pt(111) surfaces were cleaned and judged free of impurities by a standard procedure described earlier [43]. Ammonia (99.9992%), oxygen (99.998%), and hydrogen (99.9999%)

were purchased from Matheson Tri-gas, Inc. and used without further purification. The exposure of 2.0 L of O₂ at 85 K was sufficient to saturate the molecular state of oxygen (0.44 ML) on the clean Pt(111) surface as confirmed by comparison of our O₂ TPD spectra with that of others [44,45]. Saturated atomic oxygen on Pt(111) was prepared by exposing the surface to 1.0 L of O₂ at 85 K and then annealing to 300 K for 60 s. Only the high temperature O₂ desorption peak at ~750 K due to recombinative oxygen desorption was observed in the TPD experiment. An intense and sharp p(2×2) (0.25 ML) LEED pattern due to the atomic oxygen layer was observed.

3. Results

3.1. Temperature programmed desorption of NH₃/O₂/Pt(111)

Before obtaining the TPD results shown in Fig. 1, the Pt(111) crystal was exposed to 2.0 L of O₂ at 85 K followed by NH₃ exposures of 0.1 L (a) and 0.4 L (b). On clean Pt(111), a 0.1 L NH₃ exposure corresponds to a coverage of ~0.13 ML, whereas 0.4 L of NH₃ forms a bilayer [40,46]. The following desorption products were monitored: H₂ (*m/e* = 2), NH₃ (*m/e* = 17), H₂O (*m/e* = 18), N₂ (*m/e* = 28), NO (*m/e* = 30), and O₂ (*m/e* = 32). Nitric oxide (NO) was the only oxide of nitrogen observed. It is immediately clear that the desorption products observed depend on the ammonia exposure for the same nominal O₂ coverage. Hydrogen desorption is absent for both NH₃ exposures. It is completely consumed by the surface oxygen to form H₂O as shown in the *m/e* = 18 traces. Much less H₂O and N₂ are observed in

Fig. 1a than in Fig. 1b simply because less nitrogen and hydrogen are available for the lower NH₃ exposure. If all of the NH₃ is completely dehydrogenated through the reaction with O₂, then the maximum surface N atom coverage for 0.1 L NH₃ would be ~0.13 ML. However, some NH₃ desorbs (Fig. 1a trace *m/e* = 17) instead of reacting, even though there is enough surface oxygen to consume all the hydrogen from the NH₃. Some of the surface nitrogen also desorbs in the form of NO as shown in Fig. 1a. In contrast, there is no NO desorption for the higher NH₃ exposure, Fig. 1b. The area under the N₂ TPD spectrum in Fig. 1b is approximately 3.3 times larger than in Fig. 1a and the N₂ peak position shifts from 510 K for 0.1 L of NH₃ to 453 K for 0.4 L of NH₃, which is in agreement with the second-order kinetics expected for recombinative desorption. The fact that more surface nitrogen is produced for 0.4 L of NH₃ can be seen also through the increase in the amount of H₂O desorption. It is also interesting to note the differences in O₂ desorption for the two cases. First, the amount of molecular O₂ desorption is significantly lower in the case of the higher NH₃ coverage (Fig. 1b). Comparison with the desorption of 2.0 L of O₂ from clean Pt(111) indicates that the *m/e* = 32 trace in Fig. 1b represents ~22% of the initial amount of oxygen adsorbed on Pt(111). Second, the O₂ desorption peak shifts from 150 to 170 K when the NH₃ exposure is increased from 0.1 to 0.4 L. This suggests that molecular oxygen is stabilized by the presence of ammonia, in agreement with previous studies [32]. Finally, the high temperature peak due to recombinative oxygen desorption is absent in Fig. 1b, implying that the surface oxygen is completely consumed in the reaction with ammonia.

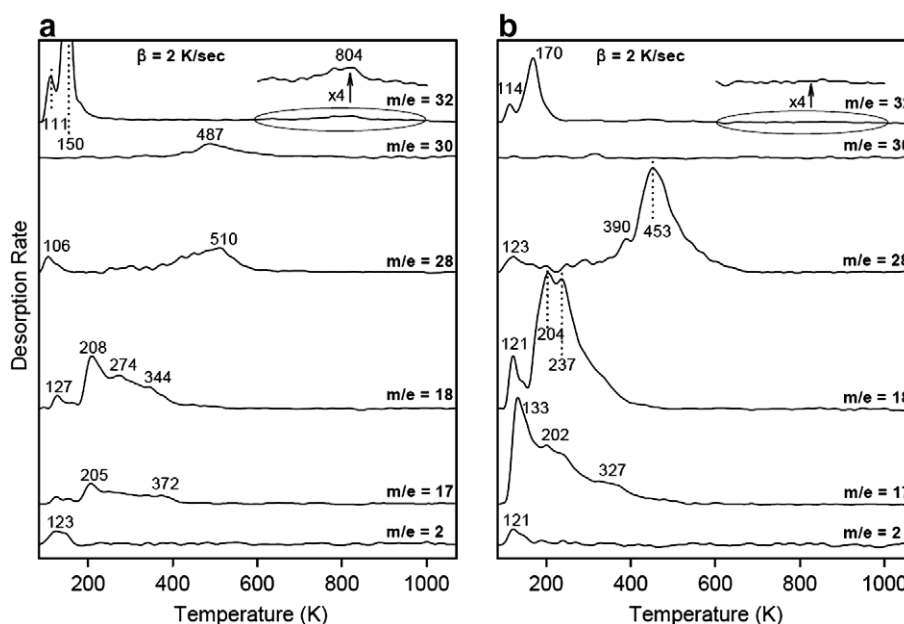


Fig. 1. TPD spectra for H₂ (*m/e* = 2), NH₃ (*m/e* = 17), H₂O (*m/e* = 18), N₂ (*m/e* = 28), NO (*m/e* = 30), and O₂ (*m/e* = 32) obtained after exposing Pt(111) at 85 K to 2.0 L of O₂ and (a) 0.1 L of NH₃, (b) 0.4 L of NH₃.

3.2. Temperature programmed desorption of $\text{NH}_3/\text{O}/\text{Pt}(111)$

Fig. 2 shows TPD results analogous to those of Fig. 1 for the case of 0.4 L of NH_3 deposited onto a $\text{p}(2 \times 2)$ atomic oxygen layer. In order to make the comparison between Figs. 1 and 2 easier, the same intensity scale is used for both. As before, hydrogen is completely consumed by the H_2O formation reaction. A flat line is observed in Fig. 2 for $m/e = 32$ showing that all atomic oxygen desorbs from the surface in the form of H_2O or NO . Two distinctive H_2O desorption peaks are present at 216 and 330 K. The stoichiometry of the reaction implies that the maximum coverage of atomic nitrogen is limited to ~ 0.17 ML, or $2/3$ of the initial O atom coverage of 0.25 ML. As expected, the N_2 TPD peak area is significantly smaller than what was observed in Fig. 1b, indicating incomplete dehydrogenation of the ammonia as also indicated by the higher amount of NH_3 desorption in Fig. 2 than in Fig. 1b. Thus, Figs. 1 and 2 reveal that a saturated O_2 layer yields more complete ammonia dehydrogenation for a given NH_3 exposure. The optimum NH_3 exposure is revealed in Fig. 3, which is a plot of N_2 TPD peak area as a function of ammonia exposure to an O_2 saturated surface. Initially the N_2 desorption increases with ammonia coverage as expected and then decreases after 0.4 L of NH_3 in part due to displacement of O_2 from the surface [32] and in part due to blocking of active sites by the excess ammonia.

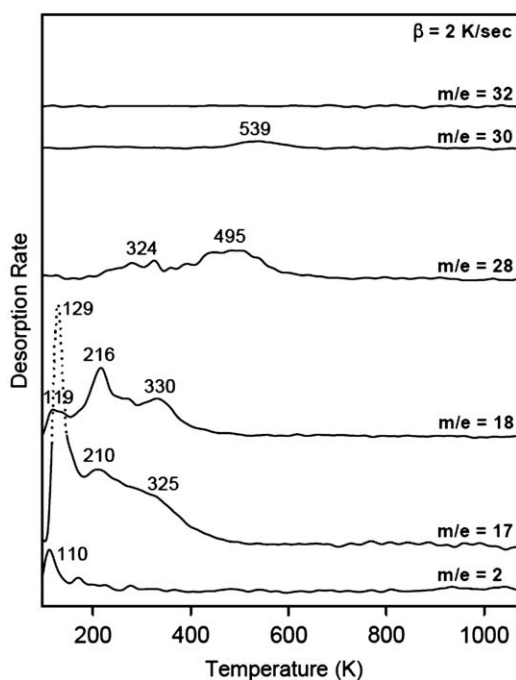


Fig. 2. TPD spectra for H_2 ($m/e = 2$), NH_3 ($m/e = 17$), H_2O ($m/e = 18$), N_2 ($m/e = 28$), NO ($m/e = 30$), and O_2 ($m/e = 32$) obtained after exposing $\text{Pt}(111)$ pre-covered with $\text{p}(2 \times 2)$ atomic oxygen to 0.4 L of NH_3 . The $\text{p}(2 \times 2)\text{-O}$ was prepared by annealing $\text{Pt}(111)$ to 300 K for 60 s following 1.0 L of O_2 exposure at 85 K.

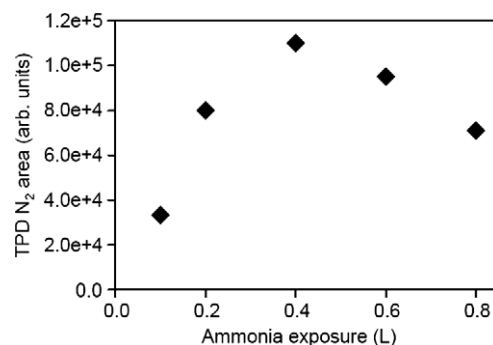


Fig. 3. N_2 TPD peak area as a function of initial NH_3 exposure on O_2 saturated $\text{Pt}(111)$. Saturated $\text{O}_2/\text{Pt}(111)$ was prepared by exposing 2.0 L of O_2 at 85 K.

3.3. Reflection absorption infrared spectroscopy of $\text{NH}_3/\text{O}_2/\text{Pt}(111)$

Fig. 4 shows RAIR spectra of the $\text{NH}_3 + \text{O}_2$ reaction. Upon exposure of 2.0 L of O_2 onto the clean $\text{Pt}(111)$ surface, a peak is observed at 874 cm^{-1} , which is readily assigned to the internal vibration of the superoxo species [45,47,48]. New features develop in the spectrum following exposure to 0.4 L of NH_3 at 85 K. At the same time, the peak at 874 cm^{-1} disappears implying that the O_2 coverage has been reduced below the RAIRS sensitivity limit. The TPD data in Fig. 1b establishes that there is still some small amount of molecular oxygen present on the surface, although the fact that it desorbs at a higher temperature

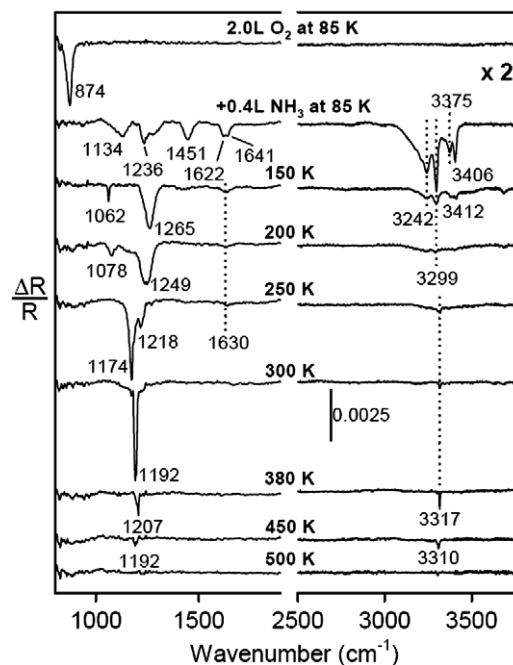


Fig. 4. RAIR spectra representing thermal evolution of $\text{Pt}(111)$ exposed to 2.0 L of O_2 and 0.4 L of NH_3 at 85 K (two upper most spectra). Before acquiring each spectrum at 85 K, the surface was annealed to the indicated temperatures. The intensity of the spectra in the $2500\text{--}3800 \text{ cm}^{-1}$ region has been multiplied by a factor of 2.

than on the clean surface indicates that it is stabilized by the presence of ammonia. Formation of an $\text{NH}_3\text{-O}_2$ complex has been suggested on $\text{Ag}(111)$ and $\text{Zn}(0001)$ [14,49] and has been discussed as an intermediate in a theoretical study of ammonia oxidation on a $\text{Cu}(111)$ surface [50]. For a 0.4 L NH_3 exposure on the clean surface, we observe peaks centered at 1617 cm^{-1} and 1211 cm^{-1} with a shoulder at 1174 cm^{-1} [40]. Because of the variety of structural arrangements assumed by the ammonia molecules even on the clean surface, a wide range of frequencies are associated with the various modes of ammonia [51]. Under slightly different conditions, Villegas and Weaver [51] assigned peaks at 1076 and 1240 cm^{-1} to $\delta_s(\text{NH}_3)$ of first layer NH_3 molecules adsorbed at threefold hollow sites on the surface and to NH_3 molecules hydrogen-bonded to first layer molecules, respectively. They also tabulated literature values for the vibrational frequencies of NH_3 in various environments, including the solid phase where $\delta_s(\text{NH}_3)$ occurs at $1058\text{--}1063\text{ cm}^{-1}$ and $\delta_{\text{as}}(\text{NH}_3)$ occurs at $1640\text{--}1646\text{ cm}^{-1}$. Therefore, we assign peaks at 1236 cm^{-1} and 1641 cm^{-1} to the symmetric and asymmetric NH_3 deformation modes. The 1134 cm^{-1} peak corresponds to the shoulder seen on the clean surface at 1174 cm^{-1} and is likewise assigned to $\delta_s(\text{NH}_3)$ of NH_3 . The 3242 cm^{-1} peak is the NH stretch of intact NH_3 and is at essentially the same position as this peak (3245 cm^{-1}) for NH_3 on clean $\text{Pt}(111)$ [40]. The peak at 1622 cm^{-1} can be attributed either to H_2O or NO , although the latter is highly unlikely since its desorption is not observed in the TPD experiment (Fig. 1b) for the conditions used in Fig. 4. In an effort to make more definitive spectral assignments of peaks that might be associated with oxygen-containing species, spectra obtained for approximately the same coverages of ammonia deposited on surfaces at 85 K covered with $^{16}\text{O}_2$ and $^{18}\text{O}_2$ are compared in Fig. 5. We assign the peak at 1641 cm^{-1} to $\delta_{\text{as}}(\text{NH}_3)$ of NH_3 and the one at 1622 cm^{-1} to $\delta(\text{HOH})$ of H_2O because no shift in the frequency of the former, but a redshift of 6 cm^{-1} for the latter, is observed upon substitution with $^{18}\text{O}_2$. This redshift is a reasonable value for the HOH bend of a water molecule. Identification of

H_2O on the surface implies that even at 85 K ammonia oxydehydrogenation is feasible, in agreement with previous studies [32]. This is confirmed by the presence of $\nu(\text{NH})$ of the NH species, an ammonia dehydrogenation product, at 3299 cm^{-1} . The peak at 1451 cm^{-1} (1433 cm^{-1} for $^{18}\text{O}_2$) is at a similar position to one observed at 1480 cm^{-1} on $\text{Ag}(111)$ that was assigned to $\nu(\text{O-O})$ of O_2 in an $\text{NH}_3\text{-O}_2$ complex [14]. The implications of Fig. 5 for spectral assignments associated with a $\text{NH}_3\text{-O}_2$ complex are considered in Section 4.

Annealing the surface decreases the intensity of all the peaks associated with NH_3 except for the most intense ones due to $\delta_s(\text{NH}_3)$ in the range of $1134\text{--}1265\text{ cm}^{-1}$. The disappearance of the NH_3 peaks is a result of both desorption and reaction with coadsorbed O_2 . The $\delta_s(\text{NH}_3)$ peaks lose their intensity dramatically above $\sim 380\text{ K}$ as shown in Fig. 4. At 150 K a new peak appears at 1062 cm^{-1} , which shifts to 1078 cm^{-1} upon annealing to 200 K . Although this peak is at a reasonable value for the bending mode of an adsorbed hydroxyl species [52], it does not shift upon $^{18}\text{O}_2$ substitution and is therefore assigned to $\delta_s(\text{NH}_3)$ of ammonia. Oxygen also reacts with the NH species as shown by a significant decrease in intensity of the peak at 3299 cm^{-1} upon annealing to 150 and 200 K . This peak shifts to 3317 cm^{-1} above 250 K and increases slightly in intensity upon annealing to 380 K due to the $\text{N} + \text{H} \rightarrow \text{NH}$ reaction. Further details on the spectroscopic characterization of the NH species on $\text{Pt}(111)$ are given in Ref. [40]. Comparison of the RAIRS results in Fig. 4 with the TPD results shown later in Fig. 9 reveals that there is a small range of temperatures between about 400 and 450 K where NH decomposes and where the resulting N atoms recombine to desorb as N_2 .

3.4. Auger electron spectroscopy of $\text{NH}_3/\text{O}_2/\text{Pt}(111)$

The AES spectra shown in Fig. 6 confirm that a nitrogen overlayer on $\text{Pt}(111)$ can be prepared free of oxygen and other contaminants. The spectra were obtained with an incident beam current of $10\text{ }\mu\text{A}$ and an energy of 3 kV . Upon adsorption of O_2 at 85 K (Fig. 6b) on the clean $\text{Pt}(111)$ surface (Fig. 6a), the oxygen KLL peak at 516 eV is observed. Although the Auger peak corresponding to surface nitrogen overlaps with one of the platinum transitions at 390 eV , the changes in this peak upon ammonia exposure clearly reveal the presence of surface nitrogen. The intensity of this peak remains essentially unchanged after annealing to 400 K , whereas the peak corresponding to the surface oxygen completely disappears (Fig. 6d). The small peak at around 273 eV is due to carbon contamination to the extent of about 2% of a monolayer. Otherwise, the surface is covered with a pure N overlayer.

3.5. Low energy electron diffraction of $\text{NH}_3/\text{O}_2/\text{Pt}(111)$

The LEED pattern shown in Fig. 7 was obtained after the $\text{Pt}(111)$ surface was exposed to 2.0 L of O_2 at 85 K ,

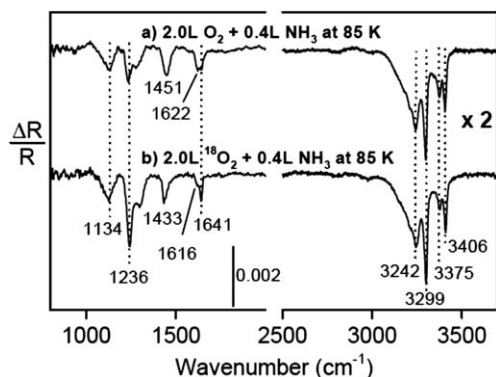


Fig. 5. RAIR spectra of $\text{Pt}(111)$ acquired after exposing (a) 2.0 L of O_2 and 0.4 L NH_3 at 85 K ; and (b) 2.0 L $^{18}\text{O}_2$ and 0.4 L NH_3 at 85 K .

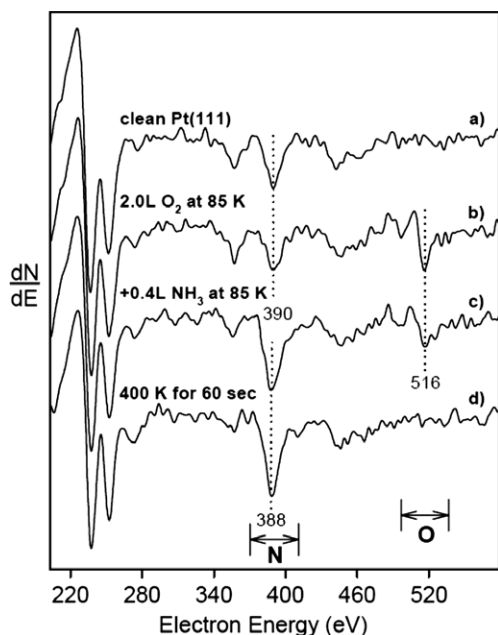


Fig. 6. AES spectra of (a) the clean Pt(111) surface, (b) after exposing the surface in (a) to 2.0 L of O_2 , (c) after exposing the surface in (b) to 0.4 L of NH_3 , (d) after annealing the surface in (c) to 400 K for 60 s.

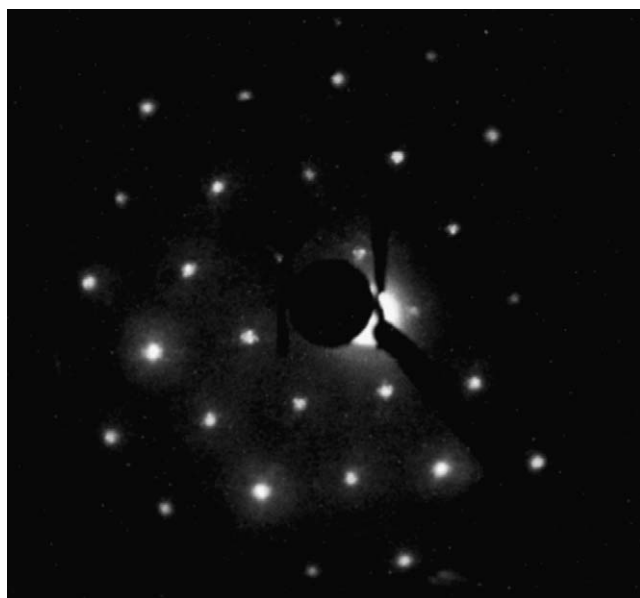


Fig. 7. LEED photograph of the $p(2 \times 2)$ -N layer on Pt(111). The surface was exposed to 2.0 L of O_2 and 0.4 L of NH_3 at 85 K followed by a 400 K anneal for 60 s before the photograph was taken.

exposed to 0.4 L of NH_3 , and then annealed to 400 K for 60 s. An intense and sharp $p(2 \times 2)$ pattern is observed in agreement with previous studies [31,32]. The $p(2 \times 2)$ pattern implies an absolute N coverage of 0.25 ML. Annealing to temperatures above 400 K led to a decrease in intensity of the $p(2 \times 2)$ spots due to desorption of nitrogen. In contrast, if the surface was annealed to only 380 K, in addition to the $p(2 \times 2)$ -N pattern weak spots due to a $(\sqrt{3} \times \sqrt{3})R30^\circ$ superstructure were observed. These

additional LEED spots originate either from a mixture of surface species present below 400 K, or from N atoms in a $(\sqrt{3} \times \sqrt{3})R30^\circ$ structure. For instance, both (2×2) and $(\sqrt{3} \times \sqrt{3})R30^\circ$ -N phases have been observed on Ru(0001), with the latter being formed at lower temperatures than the (2×2) -N phase [53].

3.6. Hydrogenation of surface N atoms to form NH: RAIRS, TPD, and XPS

Fig. 8 shows RAIR spectra of the hydrogenation of the $p(2 \times 2)$ -N structure formed by the $NH_3 + O_2$ reaction. The surface was first exposed to 2.0 L of O_2 and 0.4 L of NH_3 at 85 K followed by a 400 K anneal for 60 s and then cooled back to 85 K where spectrum (a) was taken. No peaks are observed in Fig. 8a nor were any peaks observed in the $800\text{--}2000\text{ cm}^{-1}$ region. This is consistent with a surface covered only with N atoms, where the only surface IR active mode would be well below the cutoff of our detector. For spectra (b)–(f), the surface from (a) was exposed to the indicated amount of H_2 at 300 K, annealed to 380 K, then cooled to 85 K where the spectra were obtained. For a 10 L H_2 exposure, a peak appears at 3320 cm^{-1} , which is readily assigned to $\nu(NH)$ of the NH species [40]. The NH stretch peak area continues to increase for exposures of 20, 40, and 80 L, but does not show a further increase for 160 L. The FWHM reaches its minimum value of 4.4 cm^{-1} for a 40 L exposure, but then increases for higher H_2 exposures. The fact that the NH peak area appears to

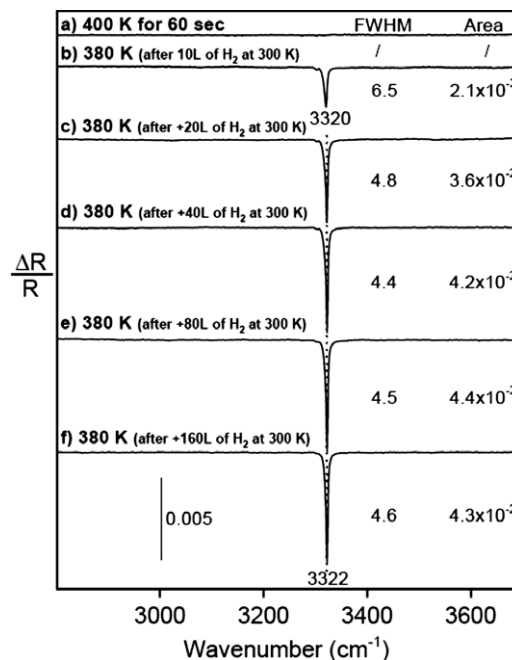


Fig. 8. RAIR spectra showing formation of the NH species. (a) Spectrum acquired at 85 K after the Pt(111) surface was exposed to 2.0 L of O_2 and 0.4 L of NH_3 at 85 K and then annealed to 400 K for 60 s. (b–f) Spectra obtained after the surface in (a) was exposed to the indicated amounts of H_2 at 300 K, annealed to 380 K for 30 s, and cooled back to 85 K.

reach a limiting value for the spectra of Fig. 8, suggests that either all of the N is converted to NH, or that the reaction has reached a limiting value for some other reason. The observed FWHM in Fig. 8d of 4.4 cm^{-1} corresponds to an intrinsic FWHM of $\sim 3.9 \text{ cm}^{-1}$, after correcting for the instrumental contribution. Such unusually narrow line widths are generally indicative of a highly homogeneous environment for the adsorbate. Although the intensity of the NH stretch peak is high, this does not necessarily imply a high NH coverage. However, independent estimates of the NH coverage can be obtained from H_2 TPD and from XPS of the N 1s region.

The TPD spectra in Fig. 9 were collected for the system represented in Fig. 8f. The only desorption products observed were H_2 ($m/e = 2$) and N_2 ($m/e = 28$). Nitrogen desorption starts at $\sim 400 \text{ K}$ as shown by the $m/e = 14$ channel, which is due to N atoms from N_2 dissociation in the ionizer of the mass spectrometer. Two peaks are present in the $m/e = 28$ desorption trace. The one centered at 481 K is due to N_2 desorption as confirmed by comparison with the $m/e = 14$ signal. The 408 K $m/e = 28$ peak is due to CO adsorbed from the background. The $m/e = 12$ signal due to C atoms from CO dissociation supports this interpretation. The H_2 TPD peak observed at 356 K consists of multiple components, and the overall H_2 desorption profile was fit with four separate peaks. These four peaks were a convolution of Lorentzian and Gaussian line shapes and the peak area, width, and peak temperature of each component was varied to give the best fit to the overall shape. The areas of these peaks can be compared to the area corresponding to a saturation coverage of hydrogen on

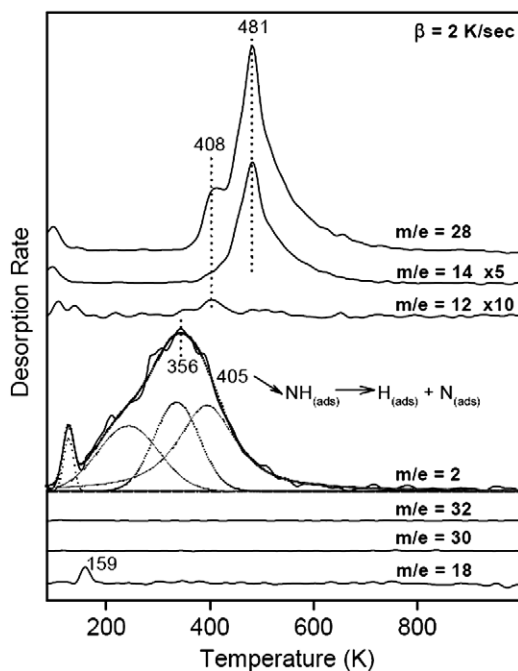


Fig. 9. TPD spectra for H_2O ($m/e = 18$), NO ($m/e = 30$), O_2 ($m/e = 32$), H_2 ($m/e = 2$), C ($m/e = 12$), N ($m/e = 14$), and N_2 ($m/e = 28$) obtained for the surface in Fig. 8f.

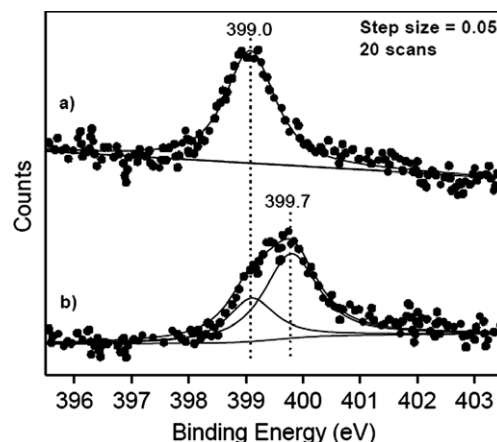


Fig. 10. The N 1s XPS peak obtained (a) after exposing 2.0 L of O_2 and 0.4 L of NH_3 to the sample at 85 K , followed by annealing to 400 K ; (b) after exposing the surface in (a) to 300 L of H_2 at 300 K and subsequent annealing to 380 K for 30 s .

$\text{Pt}(111)$ (not shown), which is known to be 1.0 ML [54]. The lowest temperature peak is due to desorption from the tungsten heating wires, rather than from the $\text{Pt}(111)$ surface. The next two components correspond to H_2 recombinative desorption of hydrogen adsorbed from the background. The combined area of these two peaks implies a hydrogen coverage of 0.17 ML from background adsorption. The highest temperature of the four peaks is centered at 405 K and is assumed to be associated with NH dissociation. The area of this peak yields an NH coverage of 0.15 ML , indicating that $\sim 60\%$ of the surface N atoms are converted to NH . However, the uncertainty in fitting the H_2 TPD area and separating the part of the H_2 desorption due to NH dissociation from the part due to background adsorption makes the uncertainty in NH coverage determined by this method rather high.

In Fig. 10 we compare XPS N 1s binding energies for the $\text{p}(2 \times 2)\text{-N}$ covered $\text{Pt}(111)$ surface (a) before and (b) after hydrogenation. In (a) the N 1s peak is well described by a single peak at 399.0 eV . Upon hydrogenation, the peak shifts to 399.7 eV and contains a low-binding-energy shoulder, indicative of incomplete hydrogenation. The two peaks fitted to reproduce spectrum (b) in Fig. 10 indicate that $\sim 68\%$ of the surface N atoms are converted to NH , in good agreement with the TPD results.

4. Discussion

The importance of the ammonia oxidation reaction over platinum catalysts has stimulated several previous surface science studies of this reaction on platinum single crystal surfaces [21,27–35]. On many points these studies are in agreement with each other and with the results presented here. Thus, in every case it is found that NH_3 is readily oxidized to H_2O , which desorbs below 400 K . In addition, NO can also be formed but is favored under oxygen rich conditions [27]. The nitrogen is removed from the surface primarily in the recombinative desorption of N_2 , which

peaks at ~ 450 K [29,32,39]. One previous RAIRS study of the reaction of NH_3 with atomic oxygen on $\text{Pt}\{100\}$ showed spectra of only one surface species, NO, but also referred to spectra not shown indicating the presence of NH_2 on the surface [35]. Our results do not offer any significant new insights into the conditions that favor NO formation, which have been a primary focus of the previous studies. Instead, we focus on the spectra of the mixed O_2/NH_3 layer and on the high reactivity of the surface nitrogen atoms towards H to form the NH species on $\text{Pt}(111)$, which has not been reported by other research groups. In the present study we are able to explore the NH formation reaction starting with a well-ordered $\text{p}(2 \times 2)$ -N layer.

Similar vibrational features that we observe for the NH_3/O_2 layer on $\text{Pt}(111)$ are also apparent in the HREEL spectra of Mieher and Ho [32]. They assigned a 1097 cm^{-1} peak to $\delta_s(\text{NH}_3)$ of second and multilayer NH_3 . Peaks at 1452 and 3371 cm^{-1} in their spectra were not specifically assigned but were also associated with an increase in NH_3 coverage. Regardless of whether an actual $\text{NH}_3\text{-O}_2$ complex forms from the interaction of O_2 and NH_3 on $\text{Pt}(111)$, as proposed by Carley et al. [14] in a study on $\text{Ag}(111)$, there are three reasons to associate the peaks we observe at 1134 , 1451 , and 3375 cm^{-1} to an interaction between O_2 and NH_3 . First, on the clean $\text{Pt}(111)$ surface at 85 K ammonia coverages ranging from submonolayer to multilayer gave no peaks at these three frequencies. Second, the peaks appeared when O_2 , but not O, was present on the surface. Third, they disappear simultaneously upon annealing the surface to 150 K (Fig. 4). The peaks at 1134 and 3375 cm^{-1} would then correspond to $\delta_s(\text{NH}_3)$ and $\nu_{\text{as}}(\text{NH})$ of an NH_3 molecule perturbed through its interaction with O_2 . However, it is not plausible to assign the peak at 1451 cm^{-1} to a perturbed ammonia peak, nor does it seem to correspond to likely reaction products such as NH_2 or OH. The $\delta(\text{NH}_2)$ mode of the NH_2 species has been ruled out as it has been reported to be at 1555 cm^{-1} on $\text{Pt}(111)$ [55] and the PtOH bending mode of OH on $\text{Pt}(111)$ has been reported to be in the range of $863\text{--}919\text{ cm}^{-1}$ [32]. The $\delta(\text{OOH})$ mode occurs at 1389 and 1380 cm^{-1} for isolated $^{16}\text{O}^{16}\text{OH}$ and $^{18}\text{O}^{18}\text{OH}$ molecules, respectively [56]. The same frequency ratio applied to the 1451 cm^{-1} peak would imply a shift to 1441 cm^{-1} , rather than to 1433 cm^{-1} as observed in Fig. 5 upon replacement of $^{16}\text{O}_2$ with $^{18}\text{O}_2$. Carely et al. [14] assigned peaks at 1480 and 1640 cm^{-1} to $\nu(\text{O-O})$ to two different forms of molecular oxygen. The assignment is strongly supported by their observation that the two peaks are in exactly the same position when NH_3 is replaced with ND_3 . A physisorbed form of molecular oxygen observed at 30 K on $\text{Pt}(111)$ has a $\nu(\text{O-O})$ value of 1543 cm^{-1} for $^{16}\text{O}_2$ and 1457 cm^{-1} for $^{18}\text{O}_2$ [47]. If the peak that we observe at 1451 cm^{-1} were also due to $\nu(\text{O-O})$ of an O_2 molecule, we would expect it to shift to approximately 1370 cm^{-1} upon replacement of $^{16}\text{O}_2$ with $^{18}\text{O}_2$. Thus the shift we observe upon $^{18}\text{O}_2$ substitution is more consistent with a $\delta(\text{OOH})$ mode rather than a $\nu(\text{O-O})$ mode of a $\text{NH}_3\text{-O}_2$

complex. Since the exact positions of such a mode for either an OOH surface species, or for a mode involving an H atom shared between O_2 and NH_3 molecules are unknown, this assignment must be tentative.

Mieher and Ho [32] identified NH_2 based on the weak peaks at 1613 , 1750 and 3306 cm^{-1} that they observed at temperatures between 285 and 380 K . They also observed a strong $\delta_s(\text{NH}_3)$ peak of ammonia at 285 K , which attenuates after annealing to 380 K , in agreement with our observations (Fig. 4). An HREELS study by Sun et al. [55] assigned losses observed at 488 , 830 , 1392 , 1555 , and 3250 cm^{-1} to NH_2 , which was produced when NH_3 on $\text{Pt}(111)$ was bombarded with 50 eV electrons. They [55] concluded that the NH_2 species is stable only to 300 K . However, even if the electron bombardment of NH_3 does produce NH_2 , the latter species is not stable at temperatures that are high enough to desorb undissociated NH_3 ; consequently, this method cannot lead to a pure NH_2 layer on $\text{Pt}(111)$. This makes definitive spectroscopic identification of NH_2 in the course of ammonia oxydehydrogenation difficult. Moreover, we have shown clearly that the peak at 3317 cm^{-1} from Fig. 4 corresponds to $\nu(\text{NH})$ of the NH species. This peak presumably corresponds to the 3306 cm^{-1} peak of Mieher and Ho [32].

One focus of this study was the formation of an N layer on $\text{Pt}(111)$ and its reactivity towards hydrogen. From Fig. 7 we know that under the conditions used here the nitrogen atoms will form a $\text{p}(2 \times 2)$ structure implying an absolute coverage of 0.25 ML . Figs. 6d and 8a confirm the absence of any other surface species and hence the high purity of the N layer on $\text{Pt}(111)$. Introduction of H_2 to the N covered surface leads to the appearance of a RAIRS peak (Fig. 8) centered at 3320 cm^{-1} , which shifts slightly to 3322 cm^{-1} for higher H_2 exposures. Comparison with our previous work on electron stimulated ammonia dissociation [40] and the absence of other vibrational modes in the spectra in Figs. 8b–f supports assignment of this peak to the NH species. The NH coverage for the conditions of Fig. 8f can be obtained from a comparison of the fraction of the H_2 desorption that occurs above 380 K to the area of the H_2 peak for a saturation coverage of H on $\text{Pt}(111)$, which is known to be 1.0 ML [54]. The comparison yields an NH coverage of 0.15 ML , indicating that only a fraction ($\sim 60\%$) of the N atoms on $\text{Pt}(111)$ can react with hydrogen to form NH. This observation is further supported by the XPS results in Fig. 10, which imply an NH coverage of 0.17 ML .

Finally, we have compared the results presented here with the results described recently involving electron-induced NH_3 dissociation on $\text{Pt}(111)$ [40]. We find that the oxydehydrogenation of ammonia through the $\text{NH}_3\text{-O}_2$ complex is a more efficient method for producing surface N atoms on $\text{Pt}(111)$. This route gives not only a well-ordered $\text{p}(2 \times 2)$ -N structure but also yields $\sim 25\%$ more atomic nitrogen on the surface. If we assume that the NH stretch peak area measured with RAIRS is proportional to the NH coverage, we find that the maximum

NH coverage achievable from hydrogenation of the $p(2 \times 2)$ -N layer is 70% higher than can be achieved from electron-induced dissociation of NH_3 . This also indicates that a higher fraction of the surface N atoms in the $p(2 \times 2)$ structure can be hydrogenated. However, it remains puzzling as to why the $p(2 \times 2)$ -N cannot be completely converted to a $p(2 \times 2)$ -NH overlayer. This would be expected since all of the N atoms are equivalent in the well-ordered structure and if any of the N atoms can be converted to NH, then all should be capable of undergoing the same reaction. This line of reasoning, however, ignores the influence of adsorbate–adsorbate interactions. In this case, repulsive interactions between NH molecules may make a complete (2×2) NH layer less energetically favorable than a mixed N and NH layer.

5. Summary

A clean well-ordered $p(2 \times 2)$ layer of N atoms on the Pt(111) surface has been prepared by dehydrogenation of ammonia with molecular oxygen. The use of molecular oxygen, as opposed to a layer of atomic oxygen, is more effective largely because a higher coverage of oxygen atoms (0.44 ML) can be achieved with molecular oxygen than with atomic oxygen, which is limited to coverage of 0.25 ML under the conditions used here. The N atoms of the $p(2 \times 2)$ -N layer are readily hydrogenated to the NH species. However, the hydrogenation reaction does not proceed beyond NH to form NH_2 or NH_3 . The H_2 TPD and the XPS results indicate that the $p(2 \times 2)$ -N layer cannot be completely hydrogenated to a $p(2 \times 2)$ -NH layer under the conditions used here. Although the maximum NH coverage achieved is difficult to quantify, it appears that less than 70% of the N atoms are converted to NH.

References

- [1] T.H. Chilton, The Manufacture of Nitric Acid by the Oxidation of Ammonia, Chemical Engineering Progress Monograph Series, No. 3, vol. 56, American Institute of Chemical Engineers, New York, 1960.
- [2] S.A.C. Carabineiro, A.V. Matveev, V.V. Gorodetskii, B.E. Nieuwenhuys, Surf. Sci. 555 (2004) 83.
- [3] H.H. Huang, C.S. Seet, G.Q. Xu, Surf. Sci. 317 (1994) 353.
- [4] M.L. Wagner, L.D. Schmidt, J. Phys. Chem. 99 (1995) 805.
- [5] T. Pignet, L.D. Schmidt, J. Catal. 40 (1975) 212.
- [6] A.K. Santra, B.K. Min, C.W. Yi, K. Luo, T.V. Choudhary, D.W. Goodman, J. Phys. Chem. B 106 (2002) 340.
- [7] S.A.C. Carabineiro, B.E. Nieuwenhuys, Surf. Sci. 532–535 (2003) 87.
- [8] S.A.C. Carabineiro, B.E. Nieuwenhuys, Surf. Sci. 505 (2002) 163.
- [9] F.P. Netzer, T.E. Madey, Surf. Sci. 119 (1982) 422.
- [10] B. Lescop, A. Galtayries, G. Fanjoux, J. Phys. Chem. B 108 (2004) 13711.
- [11] C.T. Au, M.W. Roberts, Chem. Phys. Lett. 74 (1980) 472.
- [12] B. Afsin, P.R. Davies, A. Pashusky, M.W. Roberts, D. Vincent, Surf. Sci. 284 (1993) 109.
- [13] I. Louis-Rose, C. Méthivier, C.-M. Pradier, Catal. Today 85 (2003) 267.
- [14] A.F. Carley, P.R. Davies, M.W. Roberts, K.K. Thomas, S. Yan, Chem. Commun. 1 (1998) 35.
- [15] T. Aruga, K. Tateno, K. Fukui, Y. Iwasawa, Surf. Sci. 324 (1995) 17.
- [16] C.T. Au, M.W. Roberts, Nature 319 (1986) 206.
- [17] J.J. Ostermaier, J.R. Katzer, W.H. Manogue, J. Catal. 33 (1974) 457.
- [18] B.A. Morrow, I.A. Cody, J. Catal. 45 (1976) 151.
- [19] D.P. Sobczyk, E.J.M. Hensen, A.M. de Jong, R.A. van Santen, Top. Catal. 23 (2003) 109.
- [20] C.W. Nutt, S.W. Kapur, Nature 220 (1968) 697; C.W. Nutt, S.W. Kapur, Nature 224 (1969) 169.
- [21] M. Baerns, R. Imbihl, V.A. Kondratenko, R. Kraehnert, W.K. Offermans, R.A. van Santen, A. Scheibe, J. Catal. 232 (2005) 226.
- [22] T. Pignet, L.D. Schmidt, Chem. Eng. Sci. 29 (1974) 1123.
- [23] G.S. Selwyn, M.C. Lin, Langmuir 1 (1985) 212.
- [24] M. Flytzani-Stephanopoulos, L.D. Schmidt, R. Caretta, J. Catal. 64 (1980) 346.
- [25] C.G. Takoudis, L.D. Schmidt, J. Catal. 84 (1983) 235.
- [26] M. Sheintuch, J. Schmidt, J. Phys. Chem. 92 (1988) 3404.
- [27] J.L. Gland, V.N. Korchak, J. Catal. 53 (1978) 9.
- [28] J.L. Gland, G.C. Woodard, V.N. Korchak, J. Catal. 61 (1980) 543.
- [29] M. Asscher, W.L. Guthrie, T.-H. Lin, G.A. Somorjai, J. Phys. Chem. 88 (1984) 3233.
- [30] D.S.Y. Hsu, D.W. Squire, M.C. Lin, J. Chem. Phys. 89 (1988) 2861.
- [31] T.S. Amorelli, A.F. Carley, M.K. Rajumon, M.W. Roberts, P.B. Wells, Surf. Sci. 315 (1994) L990.
- [32] W.D. Mieber, W. Ho, Surf. Sci. 322 (1995) 151.
- [33] A. Scheibe, U. Lins, R. Imbihl, Surf. Sci. 577 (2005) 1.
- [34] J.M. Bradley, A. Hopkinson, D.A. King, J. Phys. Chem. 99 (1995) 17032.
- [35] M. Kim, S.J. Pratt, D.A. King, J. Am. Chem. Soc. 122 (2000) 2409.
- [36] Ya.M. Fogel, B.T. Nadykto, V.F. Rybalko, V.I. Shvachko, I.E. Korobchanskaya, Kinet. Catal. 5 (1964) 431.
- [37] D. Burgess Jr., R.R. Cavanagh, D.S. King, Surf. Sci. 214 (1989) 358.
- [38] J.L. Gland, B.A. Sexton, J. Catal. 68 (1981) 286.
- [39] A. Fahmi, R.A. van Santen, Z. Phys. Chem. 197 (1996) 203.
- [40] E. Herceg, K. Mudiyansele, M. Trenary, J. Phys. Chem. B 109 (2005) 2828.
- [41] D.-H. Kang, M. Trenary, Surf. Sci. 470 (2000) L13.
- [42] M.E. Brubaker, M. Trenary, J. Chem. Phys. 85 (1986) 6100.
- [43] D. Jentz, H. Celio, P. Mills, M. Trenary, Surf. Sci. 341 (1995) 1.
- [44] H. Steininger, S. Lehwald, H. Ibach, Surf. Sci. 123 (1982) 1.
- [45] N.R. Avery, Chem. Phys. Lett. 96 (1983) 371.
- [46] G.B. Fisher, Chem. Phys. Lett. 79 (1981) 452.
- [47] K. Gustafsson, S. Andersson, J. Chem. Phys. 120 (2004) 7750.
- [48] J. Fan, M. Trenary, Langmuir 10 (1994) 3649.
- [49] A.F. Carley, M.W. Roberts, S. Yan, J. Chem. Soc., Chem. Commun. 4 (1988) 267.
- [50] M. Neurock, R.A. van Santen, W. Biemolt, A.P.J. Jansen, J. Am. Chem. Soc. 116 (1994) 6860.
- [51] I. Villegas, M.J. Weaver, Surf. Sci. 367 (1996) 162.
- [52] G.B. Fisher, B.A. Sexton, Phys. Rev. Lett. 44 (1980) 683.
- [53] S. Schwegmann, A.P. Seitsonen, H. Dietrich, H. Bludau, H. Over, K. Jacobi, G. Ertl, Chem. Phys. Lett. 264 (1997) 680.
- [54] K. Christmann, G. Ertl, T. Pignet, Surf. Sci. 54 (1976) 365.
- [55] Y.-M. Sun, D. Sloan, H. Ihm, J.M. White, J. Vac. Sci. Technol. A 14 (1996) 1516.
- [56] D.W. Smith, L. Andrews, J. Chem. Phys. 60 (1974) 81.